Available online at www.sciencedirect.com

SciVerse ScienceDirect

Ceramics International 38 (2012) 4685–4693

CERAMICS INTERNATIONAL

www.elsevier.com/locate/ceramint

# Printing nano $TiO_2$ on large-sized building materials: Technologies, surface modifications and functional behaviour

M. Raimondo [a,*], G. Guarini [a], C. Zanelli [a], F. Marani [b], L. Fossa [b], M. Dondi [a]

[a] *ISTEC-CNR, Institute of Science and Technology for Ceramics, Via Granarolo 64 – 48018 Faenza, Italy*
[b] *SYSTEM Spa, via Ghiarola Vecchia, 73 – 41042 Fiorano Modenese, Italy*

Received 22 November 2011; received in revised form 14 February 2012; accepted 15 February 2012
Available online 24 February 2012

**Abstract**

The industrial feasibility of large-sized, photocatalytic building materials was assessed by the adoption of suitable, fast and environmental friendly technological solutions. Nanostructured $TiO_2$ coatings can be realized by ink-jet or roller printing of nano-anatase suspensions by modifying, in one single step, the chemistry and microstructural features of products. Functional coatings must be consolidated through additional thermal steps, which necessarily entail modifications of the current production cycles of ceramic tiles. This is due to the fact that the direct functionalization of unfired ceramics is detrimental to the photocatalytic performance. The microstructure of coatings depends on deposition technologies and processing conditions. However, photoactive materials that also display superhydrophilic behaviour can be obtained by employing much lower amounts of $TiO_2$ than 1.0 g $m^{-2}$, and by annealing at temperature as low as 400–500 °C. A limited increase of the cost of products is involved, especially in the case of large-sized elements.


*Keywords:* A. Sintering; B. Microstructure-final; B. Surfaces; D. $TiO_2$; E. Functional applications

## 1. Introduction

In the field of ceramic tiles, the latest market trends encourage the production of tiles having large dimensions and ever decreasing thicknesses. Innovative technological solutions have been devised to produce ceramic slabs having surface dimensions up to 3.6 m × 1.2 m and thickness down to 3–4 mm only [1–3].

The development of porcelain stoneware large slabs, which find applications both as outdoor and indoor building and construction elements (i.e. flooring, wall covering, roofing, ventilated façades, insulating panelling, tunnel lining), has recently received significant attention [1,3], especially in combination with the functionalization of their surface, as such products provide de-soiling and de-polluting capabilities [4–7]. Photocatalytic surfaces – obtained by deposition of a titanium dioxide layer – can be considered as eco-friendly materials, able to reduce air pollution in urban areas and to prevent houses, walls, tunnels, etc. from becoming sooty and dark, thus improving environmental safety and quality of life [3,8–10]. In addition, the high hydrophilicity induced by $TiO_2$ coatings promotes a favourable wetting behaviour, enhancing both antifogging and self-cleaning performances, since the micro-droplets of condensed water spread out on the surfaces forming a continuous water layer [3,11,12].

However, some technological challenges are still to be met in view of the scaling-up of such innovative construction materials to industrial standards, so that as of today large-scale applications are still limited. The main constraints are represented by the need of:

(i) immobilizing the photocatalyst on an inert support like the ceramic surface by suitable deposition and sintering techniques [7,13];
(ii) modifying the production cycles (e.g. including an additional annealing step) in order to avoid the anatase-to-rutile phase transformation, which implies a reduction of photoactivity [14–16];
(iii) obtaining materials with lasting performances, able to preserve over time their additional functionalities in different working conditions [17,18].

* Corresponding author. Tel.: +39 0546 699721; fax: +39 0546 46381.
*E-mail address:* mariarosa.raimondo@istec.cnr.it (M. Raimondo).

0272-8842/$36.00 
doi:10.1016/j.ceramint.2012.02.051

In recent years, many papers have reported the photoinduced catalytic activity and improved wettability of $TiO_2$-coated surfaces [6,9,10]. In this context, several solutions have been evaluated to single out appropriate technologies (e.g. sol–gel processes, chemical and physical vapour deposition, thermal spraying, electron-beam evaporation), each time highlighting the role played by process and product variables in obtaining the coating structure and performance [12,19–21]. In the building sector, however, some additional constraints – i.e. wide surfaces to be processed, availability of in-line deposition techniques, output rate to be kept as high as usual, cost of the final product – represent critical points to be addressed, all of them requiring adequate, prompt, and possibly cheap technical solutions while avoiding waste of material.

In this work, nanostructured $TiO_2$ coatings were realized on porcelain stoneware large-sized slabs by using industrial technologies of deposition such as ink jet printing and roller printing. These technologies are already available in many manufacturing plants for decorative purposes. Nevertheless, in this context, they were selected for the possibility of obtaining, in one single step, the deposition of the active semiconductor and the direct microstructuring of tile surfaces. The objectives are:

(i) modelling the effect of processing variables – deposition methodology, photocatalyst amount and thermal treatments – on the coating structure;
(ii) assessing both the wetting behaviour and the photoactivity of functionalized surfaces processed in different ways;
(iii) outlining the technical advantages or drawbacks connected with the industrial scale-up of photoactive construction materials and, particularly of large-sized ones.

## 2. Materials and methods

Different porcelain stoneware surfaces were selected from the production of an industrial manufacturer (Table 1): glazed (G) and unglazed (U) tiles were sampled as semi-finished (unfired, G* and U* series) and finished products (fired, GF and UF series). All products were fully characterized as to their physical, technological and mechanical properties, as reported in a previous work [1].

A commercial nano-anatase suspension in dietylenglycol from Colorobbia (Italy) was chosen to be printed on ceramic surfaces. Its particle size distribution (Dynamic Light Scattering, Zetasizer Nanoseries Malvern Instruments), surface tension (OCA 15 Tensiometer, Data Physics Instruments) and viscosity (Bohlin C-VOR 120 rotational rheometer, both at room temperature and 80 °C) were determined. Such a $TiO_2$ suspension is 100% anatase, with average particle size of 10 nm, surface tension of about 40 mN $m^{-1}$ and viscosity values of 32 and 6 mPa s at room temperature and at 80 °C, respectively.

Nanotitania layers were deposited by means of: (a) roller printing (System Rotocolor® equipment) and (b) ink jet printing (Spectra Galaxy JA 256/80 AAA apparatus). Ink-jet printing parameters (drop size: 80 pL, drop velocity 8 m $s^{-1}$, maximum drop frequency 20 kHz) were chosen to match the rheological properties of the suspension with the instrument's technical specifications. The deposition by Rotocolor® was performed at a pilot scale by using the available in-line die box-holding cylinders. Very different amounts of anatase were used to functionalize the surfaces depending on the technique, i.e. 0.4 and 0.6 g $m^{-2}$ for ink jet printing, and from 1.4 to 4.6 g $m^{-2}$ for roller printing (Table 1). Uncoated glazed and unglazed porcelain stoneware surfaces were taken as reference.

The functionalized surfaces were processed in a different way: G* and U* samples were fired in an industrial roller kiln, at a maximum temperature of 1210 °C with a thermal cycle of 50 min, while finished products (GF and UF series) underwent annealing steps in a laboratory chamber kiln at 400, 600, 800 and 1000 °C, with a thermal cycle of about 60 min (Table 1). In any case, colourless and transparent sintered coatings were obtained (even if a change in the gloss of surfaces appeared for the highest titania loading).

Phase composition and thermal stability of $TiO_2$ layers were determined by X-Ray Diffraction (XRD, Bruker D8, LynkEye

Table 1
Sampling of porcelain stoneware surfaces, amounts of printed $TiO_2$ and thermal treatments conditions.

| | Glazed | Unglazed | $TiO_2$ amount by Rotocolor® ($g/m^2$) | $TiO_2$ amount by ink jet ($g/m^2$) | Thermal treatment conditions |
|---|---|---|---|---|---|
| Reference | G | U | | | |
| Unfired | G1* | U1* | 1.4 | – | Electric roller kiln industrial cycle 1210 °C, 50 min |
| | G2* | U2* | 2.0 | – | |
| | G3* | U3* | 3.4 | – | |
| | G4* | U4* | 3.7 | – | |
| | G5* | U5* | 4.6 | – | |
| | G6* | U6* | – | 0.4 | |
| | G7* | U7* | – | 0.6 | |
| Finished | GF1 | UF1 | 1.4 | – | Electric chamber kiln annealing from 400 °C to 1000 °C, 60 min |
| | GF2 | UF2 | 2.0 | – | |
| | GF3 | UF3 | 3.4 | – | |
| | GF4 | UF4 | 3.7 | – | |
| | GF5 | UF5 | 4.6 | – | |
| | GF6 | UF6 | – | 0.4 | |
| | GF7 | UF7 | – | 0.6 | |

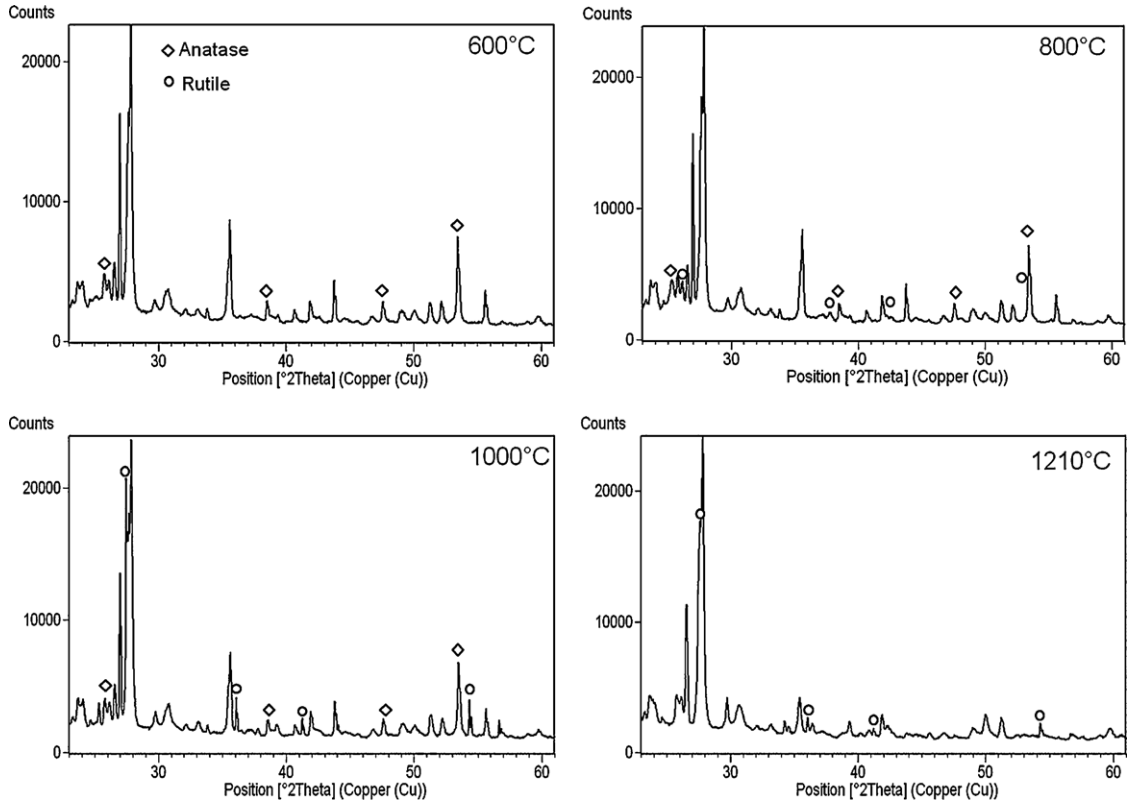


Fig. 1. Evolution of phase composition of roller printed, $TiO_2$-coated surfaces after annealing at the different temperatures and after industrial firing at 1210 °C.

detector, CuKα radiation, 10–80° 2$\theta$, 16 s of equivalent time per step) quantifying, after each thermal step, the anatase/rutile ratio by Rietveld refinement [22]. The anatase crystallite size was determined according to the Debye–Scherrer equation, taking into account the instrumental broadening by comparison with the $LaB_6$ reference material (SRM660a) [23]. The surface microstructure was investigated by SEM observations (Leica Cambridge Stereoscan 360) and by confocal microscopy (Leica Cambridge Microsystem Heidelberg Gmbh).

The wetting behaviour of the surfaces was assessed by measuring the contact angle with water (OCA 15 Tensiometer, Data Physics Instruments). For each surface, several measurements were carried out at different points on each sample, both before and after a 2-h irradiation with a UV-A lamp (OSRAM Ultra-Vitalux 300 W, light intensity 3 mW $cm^{-2}$ in the 300–400 nm range), thus yielding average values of the contact angle. Before irradiation, all samples were kept in the dark overnight.

The related experimental percent error is within 5%.

The photocatalytic activity of selected ceramic slabs, annealed at 600 or 800 °C, was determined by evaluating:

(a) the degradation of a droplet of methylene blue (MB) solution (500 ppm in water) deposited on the surface and then allowed to dry. The MB degradation index was determined by the change of absorbance (Eye-One, GretagMacbet™) before and after irradiation with the UV-A lamp for 30, 60, 120, 180 and 240 min with irradiation intensity of $2.0 \pm 0.1$ mW/$cm^2$;

(b) the progress of the oxidation of a mixture of nitrogen oxides (NO +$NO_2$) in a chamber reactor equipped with a chemiluminescence detector (experimental conditions: $NO_x$ flux: 0.03 l/min; temperature: $24 \pm 1$ °C; relative humidity: $44 \pm 5$%). Inside the reactor, samples were irradiated with a UV-A intensity of $5.0 \pm 0.1$ mW/$cm^2$, also considering the uniformity of the experimental conditions on each part of the sample. The geometry of the reactor's chamber is shown in Fig. 1.

Durability and lasting performances of coatings, in terms of wettability variations, were checked after brushing abrasion in the presence of a neutral detergent (2500 cycles). The water-coating contact angle of aged surfaces was measured after UV-A irradiation.

## 3. Results and discussion

### 3.1. Surface phase composition

According to the literature, among $TiO_2$ crystal phases anatase is thought to present enhanced photocatalytic performance because of its wider band-gap [24,25]. When considering the manufacturing of building materials and the sintering cycles currently performed, it is necessary to select processing conditions able to preserve the as-deposited anatase as the photoactive phase, by preventing both crystallite growth and anatase-to-rutile phase transformation. In fact, as it will be discussed later on in the next sections, one-step industrial firing

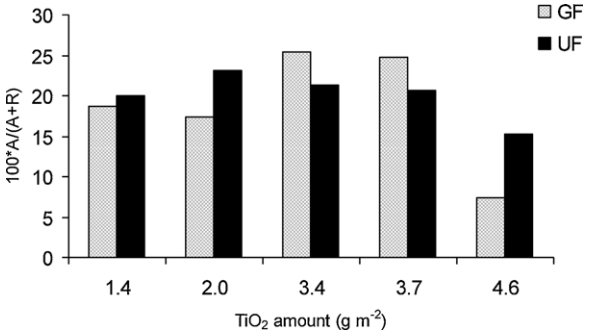


Fig. 2. [100 × Anatase/(Anatase + Rutile)] ratio in GF and UF samples after annealing at 1000 °C.

of $TiO_2$-coated green materials promotes the anatase-to-rutile conversion, with a drastic reduction or even complete loss of the desired functionalities.

In this context, the analysis of surface phase composition on samples which underwent different thermal steps allowed monitoring the anatase-to-rutile conversion (Fig. 2). The anatase/(anatase + rutile) ratio [100 × $A/(A + R)$] was subsequently quantified also as a function of the processing conditions (Fig. 3) [22]. The following conclusions can be drawn:

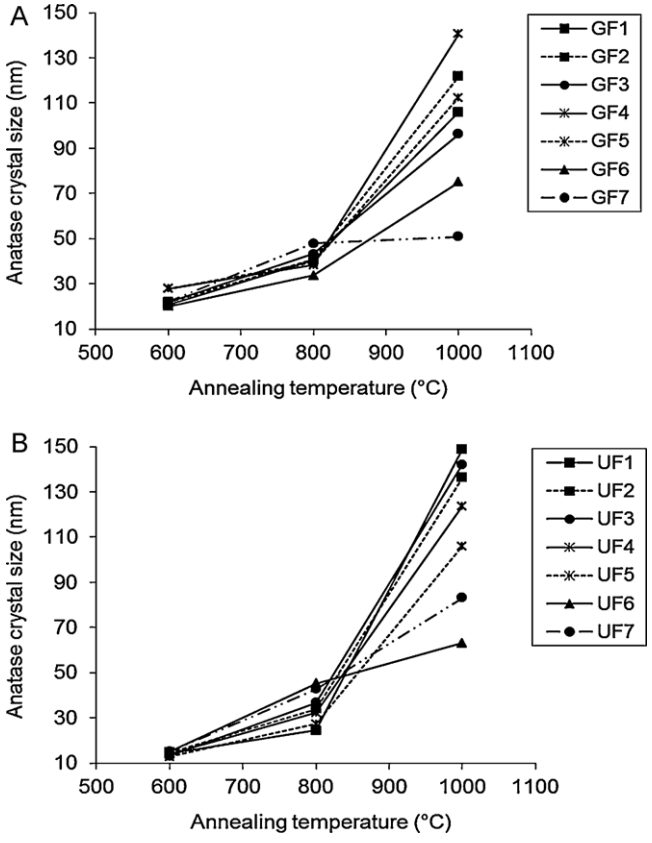


Fig. 3. Anatase crystal size evolution with annealing temperature in (A) glazed and (B) unglazed samples.

– whatever the deposition procedure and $TiO_2$ amount, anatase is the only mineralogical phase detected on both glazed and unglazed surfaces after thermal annealing up to 600 °C;
– anatase-to-rutile transformation occurs at higher temperature, but whereas at 800 °C just trace amounts of rutile are detectable, at 1000 °C the relative amount of anatase on the surface is drastically reduced, and the 100 × $A/(A + R)$ ratio reaches values between 7.4 and 25.4 for GF samples and between 15.3 and 23.1 for UF ones (Fig. 3);
– overall, glazed surfaces present a wider [100 × $A/(A + R)$] range, and the kinetics of conversion is faster when higher amounts of $TiO_2$ are deposited by using the silicone roller technology;
– a complete conversion of anatase to rutile occurs during industrial firing at 1210 °C, so rutile is the only titania phase which can be found afterwards (Fig. 2).

The evolution of the $TiO_2$ crystal size was observed from 600 °C up to 1000 °C (Fig. 4). Apart from sample typology, thermal treatments generally involve a pronounced increase of the coherent diffraction domains of anatase and some trend can be outlined. Up to 600 °C, the crystal size is in the 15–25 nm range, hence still comparable with that of the as-deposited anatase. Above 600 °C the crystallites' size increases quickly, so that at 1000 °C crystallites' dimensions are always over 70 nm. The size clearly depends on the printing technology and, as a consequence of the different titania loading, on the concentration of active particles on the surface. In the samples fired at 1000 °C, $TiO_2$ layers deposited by roller printing exhibit particle dimensions between 100 and 150 nm, while ink jet printing produces a crystal size about 70 nm.

### 3.2. Coating microstructure and morphology

SEM micrographies and confocal microscopy analyses provided evidence of a range of different structural textures of the functionalized surfaces, mainly depending on processing conditions.

SEM images of GF1 and GF6 samples obtained by roller and ink jet printing, respectively, and then thermally treated at 800 °C and 1000 °C are shown in Figs. 5 and 6. In both samples, $TiO_2$ layers mirroring the ceramic surface irregularities are detectable at high magnification. However, annealing performed at 1000 °C makes the surfaces smoother as compared to the textures obtained at 800 °C. Looking more in detail, $TiO_2$ particles appear as a flakes assemblage, whose distribution and frequency depend on the deposition technique. The flakes are larger when roller printing is used and a higher amount of $TiO_2$ is deposited (GF1 samples, Fig. 5).

These observations seem to be supported by confocal microscopy analysis (Fig. 7), which in the first place shows that the coating thickness ranges from about 70 μm (ink jet printing) to 100 μm (roller printing). In addition, whatever the annealing temperature, ink jet-printed surfaces display a more continuous coating when compared with the roller-printed ones. The comparison of surface morphology emphasizes that both printing techniques are suitable to obtain large areal

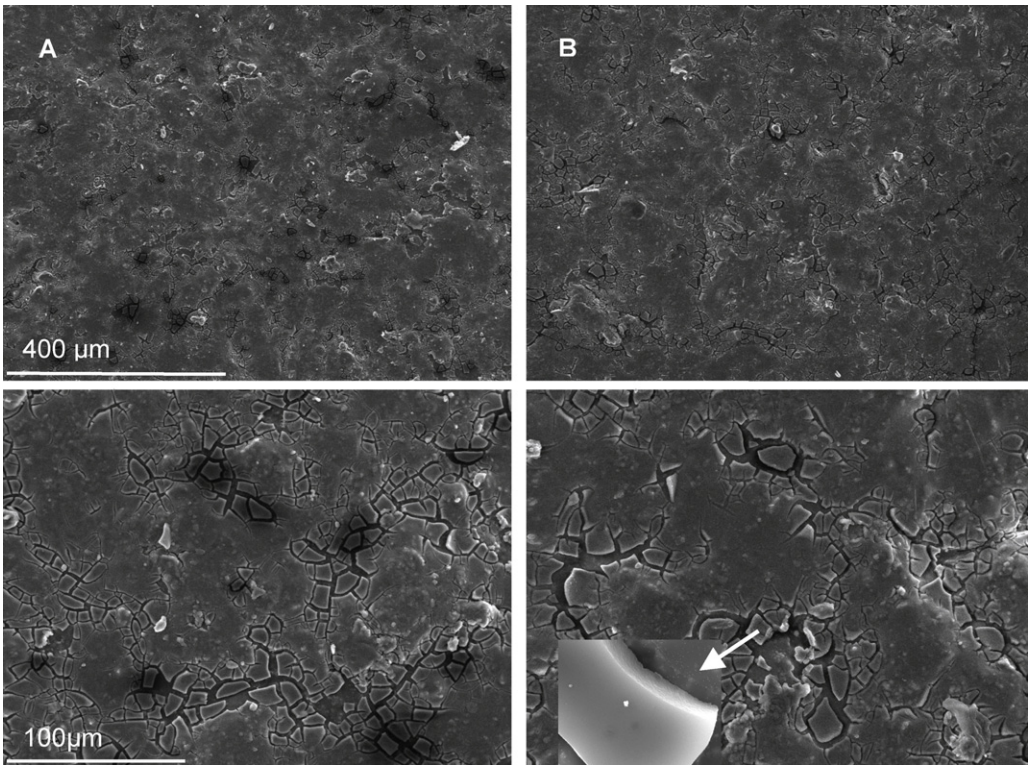


Fig. 4. SEM micrographies of GF1 sample after annealing at 800 °C (A) and 1000 °C (B) at two magnifications: 400 μm and 100 μm. A detail of $TiO_2$ flake is shown.

coverage with direct patterning of the substrates, and that $TiO_2$ amounts as low as 0.5–0.6 g $m^{-2}$ are, in every case, enough to produce textured coatings on the processed surfaces.

### 3.3. Photoinduced hydrophilicity

The wetting behaviour was assessed by measuring the contact angle (CA) of as-coated and irradiated surfaces with

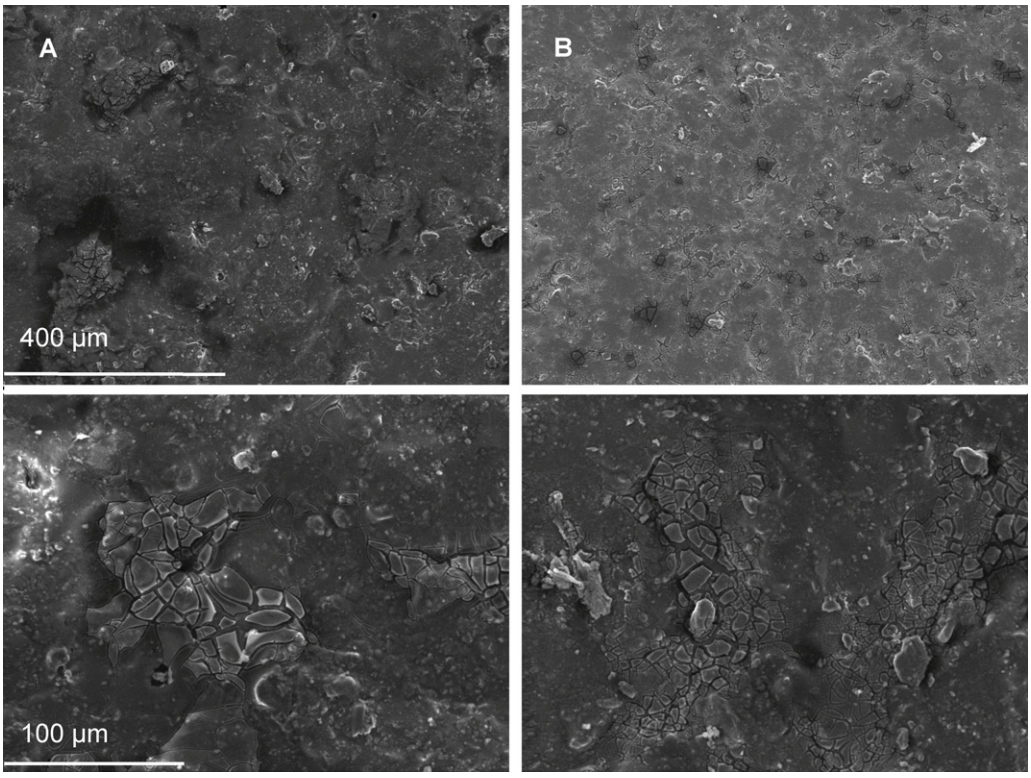


Fig. 5. SEM micrographies of GF6 sample after annealing at 800 °C (A) and 1000 °C (B) at two magnifications: 400 μm and 100 μm.

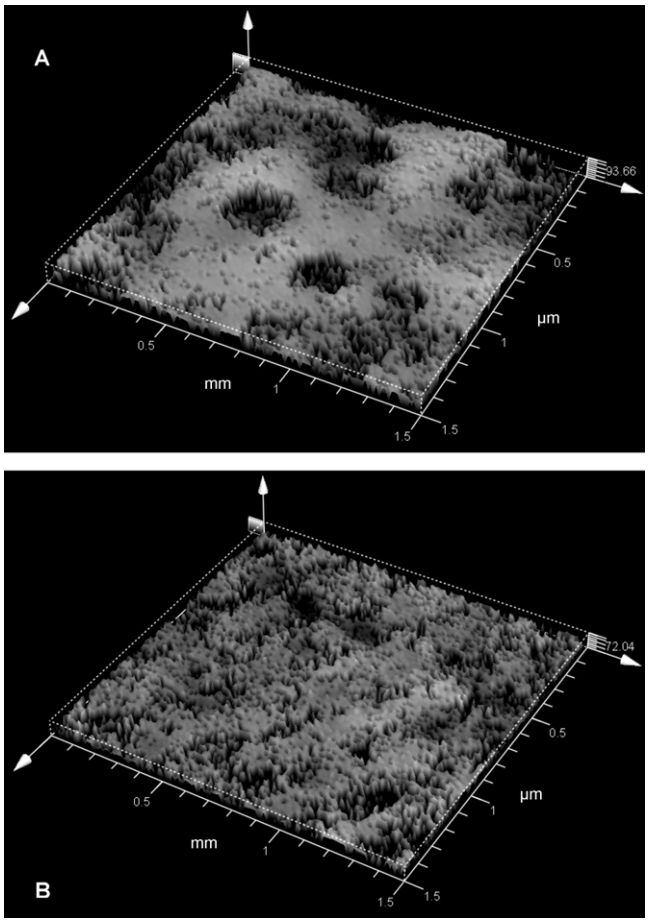


Fig. 6. Confocal microscopic images of GF1 (A) and GF6 (B) samples. *X*-axis is in mm, *Y*-axis is in μm.

water, taking the industrially manufactured uncoated slabs as reference (CA = 47° and 56° for glazed and unglazed tiles, respectively). Although, as expected, a $TiO_2$-coated surface is less hydrophilic than the uncoated one prior to any UV irradiation [11], its wettability becomes higher under UV light

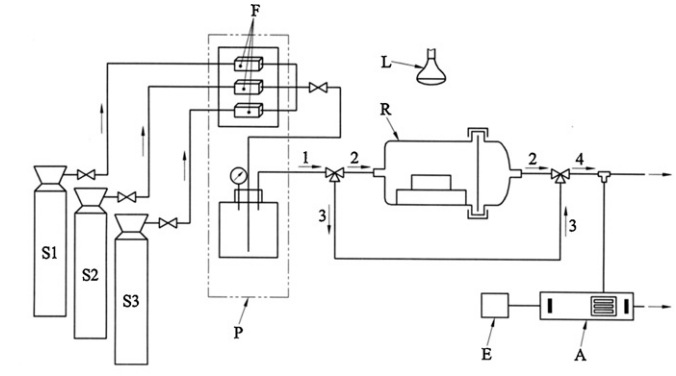


Fig. 7. Geometry of the reactor for $NO_x$ degradation.

Table 2
Wetting behaviour of $TiO_2$ as-coated surfaces by means of contact angle measurements after annealing steps (GF, UF series) or industrial firing (G*, U* series).

| | Temperature | | | | |
|---|---|---|---|---|---|
| | 400 °C | 600 °C | 800 °C | 1000 °C | 1210 °C |
| Contact angles (°) | | | | | |
| GF1 | 46 | 24 | 34 | 19 | 20 (G1*) |
| GF2 | 43 | 23 | 35 | 15 | 26 (G2*) |
| GF3 | 49 | 27 | 32 | 17 | 23 (G3*) |
| GF4 | 50 | 24 | 40 | 19 | 25 (G4*) |
| GF5 | 52 | 25 | 35 | 22 | 26 (G5*) |
| GF6 | 44 | 31 | 35 | 18 | 20 (G6*) |
| GF7 | 51 | 33 | 40 | 25 | 36 (G7*) |
| UF1 | 51 | 25 | 31 | 23 | 30 (U1*) |
| UF2 | 52 | 21 | 36 | 18 | 43 (U2*) |
| UF3 | 41 | 28 | 19 | 17 | 23 (U3*) |
| UF4 | 46 | 30 | 29 | 13 | 33 (U4*) |
| UF5 | 53 | 25 | 39 | 19 | 41 (U5*) |
| UF6 | 42 | 45 | 31 | 9 | 23 (U6*) |
| UF7 | 47 | 51 | 39 | 18 | 26 (U7*) |

Experimental error 5% relative.

by band gap excitation of the semiconductor layer [24,25]. The achievable degree of hydrophilicity depends on many factors, such as: surface texturing and microstructure, $TiO_2$ amount, layer density, etc. [11,12,20,26]. Before any UV-A exposure, the CA of water droplets on every $TiO_2$-coated sample, either glazed or unglazed, is quite depending on the thermal treatment, confirming the surface tendency towards a poor hydrophilicity (Table 2). When annealing is performed between 400 and 800 °C, CA values range from 20 to 50° for both glazed and unglazed samples. After firing at 1000 °C, the CA can be lower, but it increases again – especially in the absence of glaze – when industrial firing is performed.

As reported in the literature [27], surface wettability can change when the surface structure is altered, depending in a rather complex way on surface chemistry, roughness, type and size of crystals, etc. In this case, it could be expected that the anatase crystal growth with temperature would involve roughness variations caused by the progressive breakdown of the original surfacial nano-texture, with CA shifting toward lower values.

Upon exposure to UV-A light, the CA of samples treated up to 800 °C–both glazed and unglazed, and functionalized by both printing techniques – rapidly decreases, eventually approaching values below 5°, thus yielding superhydrophilic surfaces whereon water droplets spread out [8,10,11]. A reversal to a more hydrophobic state was also detected by storing the coated samples in the dark overnight [11] and then re-performing photoactivation and CA measurements.

Exceptions to the above findings are given by functionalized samples, which underwent either an annealing cycle at 1000 °C or industrial firing at 1210 °C. In these cases, the CA after irradiation (even when prolonged for several hours) presents values similar to those of as-coated and non-activated surfaces. This behaviour, as was expected, is due to a large extent to the anatase-to-rutile conversion which, similar to fast cycling of

ceramic tile kilns, took place over a wide thermal interval between 600 and 1200 °C, even though the maximum rate of phase transition is found around 900–1000 °C.

Overall, according to these results, it can be claimed that ink jet printing is suitable for obtaining photoactive, top-layered structured materials with enhanced attitude to link water molecules by employing very low amounts of $TiO_2$. This involves – as a key issue – a very limited increase of the cost of the functionalized products, especially when the process is applied to large-sized elements.

On the other hand, the Rotocolor® equipment itself can find extensive applications beyond decoration in the control of surface wettability through the deposition of nano-suspensions. This is due to both process speed and easiness of cleaning operations, which allow easy management of different suspensions.

### 3.4. Photocatalytic activity of ceramic surfaces

#### 3.4.1. Methylene blue degradation

The degradation of organic dyes by $TiO_2$ particles represents one of the most widely used methodology to assess the photocatalytic efficiency of materials under UV light [28]. However, the efficiency of the method depends on many factors, such as the nature, quantity and concentration of the adsorbed dye [28–30]. Among the many organic dyes proposed for such purpose, the methylene blue (MB) test is becoming a widely used method for characterizing the activity of $TiO_2$ layers, since MB has a strong staining power, thus representing a quite severe test for the photo-oxidation ability of semiconductors.

According to the previous results, two representative $TiO_2$-coated surfaces – annealed at either 600 or 800 °C – were chosen, and their activity in MB degradation compared with that of the uncoated material. The results are summarized in Fig. 8, where the percentage of MB degradation has been plotted vs. duration of irradiation. The degradation efficiency of coated samples is very high when compared with that of the uncoated ones, but the process kinetics depends on the annealing conditions. The MB degradation by the sample treated at 600 °C reaches values close to 90% after just 30 min

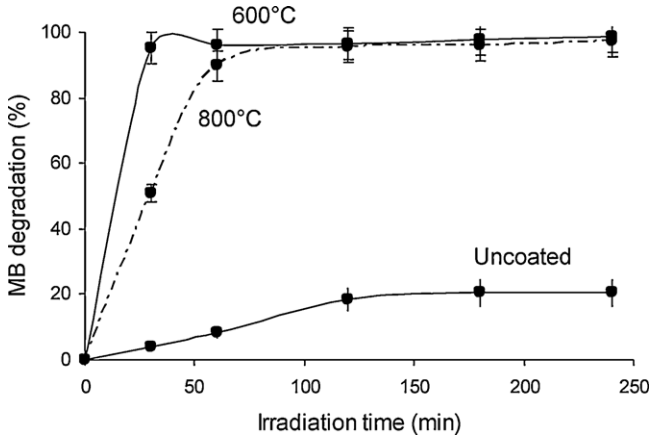


Fig. 8. Degradation of methylene blue solution by samples annealed at 600 °C and 800 °C as a function of irradiation time: comparison with the uncoated one.

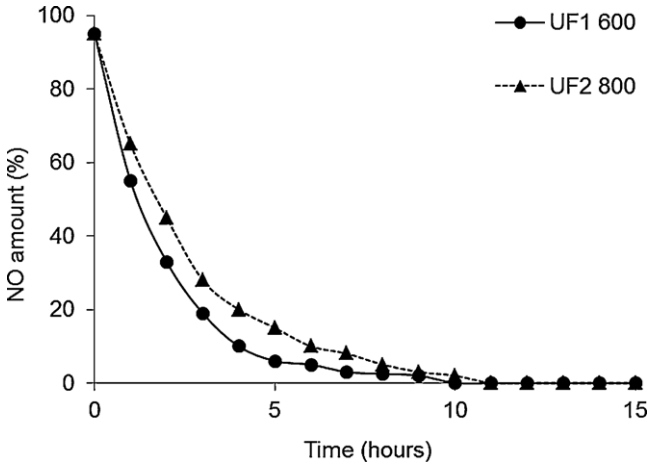


Fig. 9. Degradation of nitrogen oxide (NO) performed by samples annealed at 600 °C and 800 °C vs time.

of irradiation, and is virtually completed after about 1 h. On the other hand, the sample treated at 800 °C, although able to promote a complete degradation of dye after about 1 h, displays some inertia as regard to its activation.

#### 3.4.2. de-$NO_x$ activity

The activity of the same surfaces described in the previous section towards the oxidation of NO and $NO_2$ is illustrated in Figs. 9 and 10. Both exhibit a rather high reactivity in the adopted experimental conditions, causing an up to 95% degradation of $NO_x$ concentration. In this context, however, some differences can be outlined:

(i) overall, the degradation kinetics of nitrogen monoxide is faster if compared with that of nitrogen dioxide;
(ii) the sample treated at a lower temperature (UF1, 600 °C) confirmed to be more reactive than that treated at 800 °C. In particular, NO degradation was almost complete after 6–8 h, while for nitrogen dioxide the same level of degradation was only achieved after about 28 h (Fig. 9).

These results, combined with those concerning organic dye degradation, suggest that the kinetic of photoactivity is

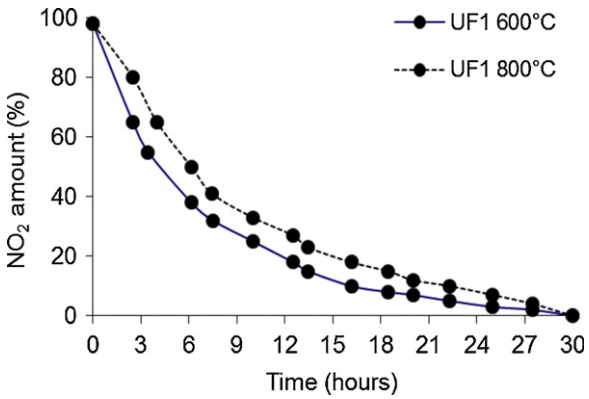


Fig. 10. Degradation of nitrogen dioxide ($NO_2$) performed by UF1 samples annealed at 600 °C and 800 °C vs time.

Table 3
CA of surfaces under UV irradiation before and after ageing.

| Sample | Contact angles (°) | |
|---|---|---|
| | Before | After |
| UF4 400 °C | <5 | 24 |
| UF4 800 °C | <5 | 22 |
| UF5 400 °C | <5 | 26 |
| UF5 800 °C | <5 | 9 |
| UF6 400 °C | <5 | 34 |
| UF6 800 °C | <5 | 24 |

correlated to both the anatase/rutile ratio and the extent of anatase crystal growth. These two phenomena take place when the temperature increases: surface activity lowers when rutile is formed and anatase crystallite dimensions increases. As a consequence, the degradation process is expected to stop once the anatase-to-rutile conversion is complete.

### 3.5. Durability and lasting properties of surfaces

The durability of coated surfaces represents a critical point, since predicting their lasting performances in different working conditions (in terms of mechanical resistance, chemical stability and residual photoactivity over time) is quite a hard task. Whilst designing such new materials, it is possible to test under specific experimental conditions the response of the coating to ageing factors, which can be simulated at the laboratory scale by abrasion tests.

Summarizing the behaviour of functionalized samples after such a brushing treatment (Table 3), it can be seen that enhanced wettability (and hence the superhydrophilic performance) can to some extent be preserved when higher amounts of $TiO_2$ are deposited, and annealing is performed at higher temperatures. This is the case of the UF5 sample, functionalized by roller printing through the deposition of 4.5 g $m^{-2}$ of $TiO_2$ and thermally treated at 800 °C, whose wettability after ageing is still acceptable due to the improved resistance of the coating to mechanical wear. Under these processing conditions, the coating adhesion is ensured and the performances kept to an adequate level notwithstanding the anatase-to-rutile conversion that begins to take place when the temperature increases. This is made clear by considering the wettability of the UG4 surface, whose lower amount of $TiO_2$ per unit area produces a worse performances against abrasion. A similar behaviour is displayed by the sample UF6, obtained by ink jet deposition of 0.6 g $m^{-2}$ of $TiO_2$.

## 4. Conclusions

The production of large-sized, photoactive building materials is feasible at the industrial scale through the adoption of suitable, fast and environmental friendly technological solutions, which in many cases are already available as in-line decoration equipment. Nanostructured $TiO_2$ coatings can be deposited by ink-jet or roller printing of nano-anatase suspensions thus modifying, in a single step, the chemical and microstructural parameters of surfaces. Such coatings need to be consolidated through an additional thermal step which, even though implying a significant modification of current production cycles of ceramic tiles, represents the proper solution to both preserve the active phase and keep mechanical and functional performances to an adequate level. At all events, a direct functionalization of unfired ceramics seems not to be feasible, because the high sintering temperature (around 1200 °C) is detrimental to the photocatalytic performance.

Deposition technologies and thermal conditions both affect the nanotitania texturing in terms of thickness, homogeneity and particle size. Product characteristics and photoactivity indicate that ink-jet printing is suitable to obtain photoactive, top-layered, structured materials with enhanced attitude to link water molecules (CA below 5°), employing $TiO_2$ amounts as low as 0.4 g $m^{-2}$. The latter entails a limited cost increase of the final products, especially when large-sized elements are concerned. On the other hand, this work suggests that roller printing can find an extensive application in the control of surface photoactivity, due to the die box-holding cylinders ability to apply $TiO_2$ nanosuspensions in a controlled way. The high speed and flexibility of the deposition process makes this technology an excellent tool for surface functionalization.

## Acknowledgements

The authors acknowledge Prof. Paolo Zannini (Chemistry Department-University of Modena and Reggio Emilia, Italy) for confocal microscopic analyses, Dr. Giovanni Baldi (Colorobbia Italia, Sovigliana Vinci (FI)) for helping in the assessment of the photocatalytic activity of the samples and dr. Carlo Baldisserri (ISTEC CNR).

## References

[1] M. Raimondo, M. Dondi, C. Zanelli, G. Guarini, A. Gozzi, F. Marani, L. Fossa, Processing and properties of large-sized ceramic slabs, Bol. Soc. Esp. Ceram. V. 49 (2010) 289–296.
[2] D. Vivona, F. Piccinini, Low thickness for large eco-efficient size, Ceram. World Rev. 83 (2009) 96–100.
[3] M. Raimondo, C. Zanelli, G. Guarini, M. Dondi, F. Marani, L. Fossa, Innovative porcelain stoneware slabs (Lamina®): from processing to applications, Proceedings of 11th International Conference on Advanced Materials 2009, Rio de Janeiro (Brasil) 20–25 (2009) 78–83.
[4] J. Chen, C.S. Poon, Photocatalytic construction and building materials: from fundamentals to applications, Build. Environ. 44 (2009) 1899–1906.
[5] R. Benedix, R. Dehn, J. Quaas, M. Orgass, Application of titanium dioxide photocatalysis to create self-ckleaning building materials, Lacer 5 (2000) 157–198.
[6] D.M. Tobaldi, A. Tucci, G. Camera-Roda, G. Baldi, L. Esposito, Photocatalytic activity for exposed building materials, J. Eur. Ceram. Soc. 28 (2008) 2645–2652.
[7] F. Bondioli, R. Taurino, A.M. Ferrari, Functionalization of ceramic tile surface by sol–gel technique, J. Coll. Int. Sci. 334 (2009) 195–201.
[8] A.L. Linsebigler, G. Lu, J.T. Yates JT Jr., Photocatalysis on $TiO_2$ surfaces: principles, mechanism and selected results, Chem. Rev. 95 (1995) 735–758.
[9] T. Maggos, J.G. Bartzis, M. Liakou, C. Gobin, Photocatalytic degradation of $NO_x$ gases using $TiO_2$-containing paint: a real case study, J. Hazard. Mater. 146 (2007) 668–673.

[10] X. Zhao, Q. Zhao, J. Yu, B. Liu, Development of multifunctional photoactive self-cleaning glasses, J. Non-Cryst. Solids 354 (2008) 1424–1430.
[11] T. Shibata, N. Sakai, K. Fukuda, Y. Ebina, T. Sasaki, Structural photoinduced hydrophilicity of titania nanosheet film, Mater. Sci. Eng. B 161 (2009) 12–15.
[12] P. Eimachai, P. Chindaudom, M. Horprathum, V. Patthanasettakul, P. Limsuwan, Design and investigation of photo-induced super-hydrophilic materials for car mirror, Mater. Design 30 (2009) 3428–3435.
[13] P. São Marcos, J. Marto, T. Trindadae, J.A. Labrincha, Screen-printing of $TiO_2$ photocatalytic layers on glazed ceramic tiles, J. Photochem. Photobiol. A: Chem. 197 (2008) 125–131.
[14] R.A. Spurr, H. Myers, Quantitative analysis of anatase–rutile mixtures with an X-ray diffractometer, Anal. Chem. 29 (1957) 760–767.
[15] P.I. Gouma, M.J. Mills, Anatase-to-rutile transformation in titania powders, J. Am. Ceram. Soc. 84 (2001) 619–622.
[16] H. Zhang, J.F. Banfield, Phase transformation of nanocrystalline anatase-to-rutile via combined interface and surface nucleation, J. Mater. Res. 15 (2000) 437–448.
[17] M. Piispanen, J. Matta, S. Areva, A.M. Sjoberg, M. Hupa, L. Hupa, Chemical resistance and cleaning properties of coated glazed surfaces, J. Eur. Ceram. Soc. 29 (2009) 1855–1860.
[18] A. Chabas, T. Lombardo, H. Cachier, M.H. Pertuisot, K. Oikonomou, R. Falcone, M. Verità, F. Geotti-Bianchini, Self cleaning versus float glass in urban atmosphere, Glass Technol.-Eur. J. Glass Sci. Technol. Part A 50 (2009) 139–142.
[19] Z. Yi, J. Liu, W. Wie, J. Wang, S.W. Lee, Photocatalytic performance and microstructure of thermal-sprayed nanostructured $TiO_2$ coatings, Ceram. Int. 34 (2008) 351–357.
[20] N. Arconada, A. Durán, S. Suárez, R. Portela, J.M. Coronado, B. Sánchez, Y. Castro, Synthesis and photocatalytic properties of dense and porous $TiO_2$-anatase thin films prepared by sol–gel, Appl. Catal. B: Environ. 86 (2009) 1–7.
[21] M. Arin, P. Lommens, N. Avci, S. Hopkins, K. De Buysser, I.M. Arabatzis, I. Fasaki, D. Poelman, I. Van Driessche, Inkjet printing of photocatalytically active $TiO_2$ thin films from water based precursor solution, J. Eur. Ceram. Soc. 31 (2011) 1067–1074.
[22] PC-APD Automated Powder Diffraction Software Operation Manual, 4th ed., Philips Analytical Eindhoven, Netherland, April 1992, Chapter 11, p. 11.
[23] F.W. Jones, Particle size measurement by the X-ray method, J. Sci. Instrum. 18 (1941) 157–158, DOI:10.1088/0950-7671/18/7/314.
[24] A. Fujishima A, T.N. Rao, D.A. Tryk, Titanium dioxide photocatalysis, J. Photochem. Photobiol. C: Photochem. Rev. 1 (2000) 1–21.
[25] A.L. Linsebigler, G. Lu, J.T. Yates, Photocatalysis on $TiO_2$ surfaces: principles, mechanisms and selected results, Chem. Rev. 95 (1995) 735–758.
[26] F. Dong, W. Zhao, Z. Wu, S. Guo, Band structure and visible light photocatalytic activity of multi-type nitrogen doped $TiO_2$ nanoparticles prepared by thermal decomposition, J. Hazard. Mater. 162 (2009) 763–770.
[27] T. Watanabe, Wettability of ceramic surfaces – a wide range control of surface wettability form superhydrophilicity to superhydrophobicity, from static wettability to dynamic wettability, J. Ceram. Soc. Jpn. 117 (2009) 1285–1292.
[28] A. Mills, M. McFarlane, Current and possible future methods of assessing the activities of photocatalyst films, Catal. Today 129 (2007) 22–28.
[29] U.G. Akpan, B.H. Hameed, Parameters affecting the photocatalytic degradation of dyes using $TiO_2$-based photocatalysis: a review, J. Hazard. Mater. 170 (2009) 520–529.
[30] S. Rehman, R. Ullah, A.M. Butt, N.D. Gohar, Strategies of making $TiO_2$ and ZnO visible light active, J. Hazard. Mater. 170 (2009) 560–569.